Case Studies in Thermal Engineering 28 (2021) 101443

Contents lists available at ScienceDirect

Case Studies in Thermal Engineering

journal homepage: www.elsevier.com/locate/csite

Thermoelastic responses in rotating nanobeams with variable physical properties due to periodic pulse heating

Ahmed M.H. Yahya [a], Ahmed E. Abouelregal [a,b,*], K.M. Khalil [a], Doaa Atta [c,d]

[a] Department of Mathematics, College of Science and Arts, Al-Qurayat, Jouf University, Saudi Arabia
[b] Basic Sciences Research Unit, Jouf University, Saudi Arabia
[c] Department of Mathematics, College of Science, Qassim University, P.O. Box 6644, Buraydah, 51482, Saudi Arabia
[d] Department of Mathematics, Faculty of Science, Mansoura University, Mansoura, 35516, Egypt

ARTICLE INFO

Keywords:
Nanobeams
Thermoelasticity
MCS theory
Centrifugal force
Changeable properties

ABSTRACT

Recently, many researchers have been interested in the so-called theories of nonlocal elasticity (NET) and modified couple stress (MCS). The effect of size and dependence on the micron scale was predicted using this theory. A new set of equations was created that governs this theory including the equation for a couple of moments and the use of the concept of couple stress elasticity. Also, the generalized thermoelastic model with phase lag is used. The present work concentrated on introducing thermoelastic rotating nanobeams structural analysis under periodic pulse heating by applying the non-local MCS theory and generalized thermoelastic theory. The thermal conductivity of the material is considered to be variable and linearly dependent on changes in temperature. Laplace transform and state space methods are used to obtain the physical fields of the nanobeam. The effects of size and non-local factors, variability of thermal conductivity, centrifugal force due to rotation and couple stress on different field variables are visually presented and examined in depth.

1. Introduction

During the last decades, micro-electrical, chemical, and biomedical technology have been attractive features for a large number of researchers. This technology refers to small mechanical and electrical components that are produced using precision production techniques. Micro-sensors, safety devices for microscopes, micro-activators, micro-resonators, energy harvesting, the use of optical metamaterials, and atomic force microscopes are major uses of MEMS technology [1]. Static and dynamic analysis should be used in the idealized models in order to provide excellent prototypes for the industrial society. It shows that classical mechanics cannot produce valid results for such small-scale systems. On the other hand, size-dependence phenomena may be captured using non-classical theories, leading to more accurate results and analysis [2].

Studies reveal a better stiffness and strength of materials than bulky materials in the micron and submicron scale. This phenomenon is known as the impact of size or scale. There are no intrinsic material length scale parameters for conventional connected mechanical theories, which cannot describe size effects. Researchers have been encouraged to create a variety of higher-order continuum theories including micropolar theory, couple stress theory, strain gradient theory, nonlocal elasticity theories and modified couple stress theory [3–9]. Some researchers have experimentally discovered the size-dependent deformation and vibrational behavior of microstructures.

* Corresponding author. Department of Mathematics, College of Science and Arts, Al-Qurayat, Jouf University, Saudi Arabia.
E-mail address: ahabogal@gmail.com (A.E. Abouelregal).

https://doi.org/10.1016/j.csite.2021.101443
Received 17 July 2021; Received in revised form 27 August 2021; Accepted 10 September 2021
Available online 20 September 2021

These experiments demonstrated that while analyzing microbeams, size-dependent behavior must be taken into account.

In recent years, nonlocal microbeam models have gained great popularity. Eringen [10,11] introduced the idea of non-local continuity mechanics to deal with issues of small-scale structural materials. Based on the complete assumption that stress anywhere is a function of strains at the same point, Eringen and Edlin [12] established a constitutive relationship to the non-local stress at any point in an integral form. The force between atoms and the internal length scale, which are taken into account in the constituent equations as a physical property, is necessary for the proposed non-local elasticity theory. Elastic wave lattice scattering, nanomechanics, wave propagation in composites, fracture mechanics, surface stress fluids, and separation mechanics are some of the applications investigated using the non-local elasticity theory [13].

The couple stress theory (CST), established by Koiter [9] and others such as Toupin [8], Mindlin and Tiersten [7], and Mindlin [14], is a higher-order continuum theory that attempts to describe the observed size-dependency of deformation in some materials, especially on the micron scale Couple stresses in the study of mechanical behavior in this model arise from continuous media, and thus the basic concepts of stress that serve to understand classical elasticity theory are inadequate. As a result of the couple stress contribution, additional elastic material constants that reflect the length of the material's intrinsic property are the constituent equations of the theory. Two constants of matter are incorporated into the linear property theory. Yang et al. [15] proposed a modified couple stress theory with only one additional length scale component due to problems in finding the material length scale parameters.

The modified couple stress theory (MCST) is widely used to describe microstructure influences with only one material length scale parameter, whereas the Gurtin–Murdoch surface elasticity theory with three surface elasticity constants is applied to approximate the nature of surface energy impacts. Hadjesfandiari and Dargush [16,17] investigated the recently created skew-symmetric couple stress theory (CST) in order to show its internal consistency, natural simplicity, and basic connection to classical mechanics. In Ref. [17], they have considered both the theoretical and practical elements of the various couple stress theory. They also discovered that the MCST not only has contradictions, but it also cannot adequately describe certain simple deformations, such as pure bending of a plate and pure torsion of a circular bar. Based on the MCST theory and the surface elasticity model of Gurtin and Murdoch, Yin et al. [18] developed an effective isogeometric Timoshenko beam model that incorporates both microstructure and surface energy effects. Based on the aforementioned non-classical theory and MCST theory, many researchers have studied static and dynamic analysis of micro and nanosystems [19–28].

Rotating nanobeams are used in a variety of nanoscale devices, and correctly modeling and studying them is a difficult challenge. Micro-cantilever contact type sensors, micro gyroscopes, micro motors, biosensors and atomic force microscopes are widely used in communications and information technology, materials characterization, chemistry, environmental monitoring, biomechanics, aerospace and the military. The main components of most miniature structures are the rotating components. As a result, researchers are fully interested in rotational effects [29].

To investigate the effects of size dependence on flapwise vibrations of rotating microbeams, Dehrouyeh-Semnani [30] established the nonclassical Euler-Bernoulli and Timoshenko beam elements. Ghadiri and Shafiei [31] investigated the thermal vibration of rotating FG Timoshenko microbeams in highly temperature-varying environments. Narendar [32] used the nonlocal theory to model the rotating SWCNT using the Euler–Bernoulli beam model. Ghadiri et al. [34] used the differential quadratic-element technique to examine the size-dependent vibration behavior of a rotating functionally graded (FG) tapered microbeam based on the modified couple stress theory.

Using a differential transformation method, Ghafarian and Ariaei [35] investigated the free vibration of a system of Timoshenko's rotating tapered beams flexibly linked with two distinct boundary conditions. To investigate the free vibration behavior of pre-twisted tapered rotating micro beams constructed from bidirectional functionally graded material (BFGM), Bhattacharya and Das [36] proposed an improved mathematical model. A large number of researchers using different solving methods have investigated the analysis of beam vibration with rotation effects [37–43].

Biot [44] proposed the theory of coupled thermoelasticity to avoid the inconsistency inherent in the conventional uncoupled model, which states that deformation changes have no effect on the temperature field. The heat conduction equations for the coupled and uncoupled models are of the diffusion type, which means that thermal waves will propagate at infinite rates, which does not correspond to physical occurrences. By incorporating thermal relaxation times into the governing relations, the coupled thermoelasticity theory has been modified by the proposal of Lord and Shulman (LS) [45] and Green and Lindsay (GL) [46] theories.

In recent years in the field of thermoplasticity, the Tzou model [47–49] is one of the latest models to gain popularity. Tzou developed the dual-phase lag model (DPL) to account for the impacts of microscopic interactions in the rapid transition of the heat transfer mechanism to microscopic in this proposal [47–49]. In addition, two different phase delays are introduced into the constitutive relationship between heat flow and temperature gradient in this approach. Recently, some new work in piezo-thermoelastic or thermoelastic materials based on generalized models of thermoelasticity has been discussed in Refs. [50–53].

The innovative theory of control is based on state-space techniques. The ability to characterize basic methods using differential equations in favor of transport functions is a major benefit of state-space methodologies. This may seem like a throwback to a simpler time when differential equations were used to express dynamic operations [22]. However, in the past, the processes were simple enough that they could be solved using only one low-order differential equation. To answer various issues in thermoelasticity theory, the potential function approach is commonly used. However, there are a number of drawbacks to this approach [54,55].

The current study is devoted to introducing a modified thermoelastic model that demonstrates the size-dependent vibration of Euler–Bernoulli microbeams considering the effects of rotation and temperature change. The model was derived by incorporating the nonlocal scale effects and based on nonlocal elasticity theory and modified couple stress model as well as the generalized thermoelasticity theories with phase lag. According to the authors' best knowledge, this is the first model of its kind that has been proposed in this field. Moreover, the novelty of the proposed work and its contribution to this paper is that it takes into account that the thermal

properties of the material are variable and depend on temperature changes.

As an application to the presented model, thermal vibrations in simply supported rotating nanobeams with variable properties are investigated. Analytical solutions for the studied field variables were derived using Laplace transform method and state-space technique. The effects of variable key factors including material length scale, rotational velocity, thermal conductivity variation, and pulse heating on nanobeam responses are investigated. The results can be used in the next generation of nanomachine research and design, such as nanoparticle bearings, nanoturbines, and nanogems, etc.

2. Nonlocal model of thermoelasticity

According to the nonlocal elasticity theory of Eringen [8–10], the stress field at a point $\boldsymbol{x}$ in an elastic continuum depends not only on the stress field at the point but also on the stress at all other points of the body. In this theory, the nonlocal stress-tensor τ_{ij} at any point $\boldsymbol{x}$ in a body can be expressed as

$$\tau_{ij}(\boldsymbol{x}) = \int_V K_1(|\boldsymbol{x},\boldsymbol{x}'|,\xi)\sigma_{ij}(\boldsymbol{x}')\mathrm{d}V(\boldsymbol{x}'), \tag{1}$$

where $\sigma_{ij}(\boldsymbol{x}')$ is the classical local stress tensor which is given by

$$\sigma_{ij}(\boldsymbol{x}') = 2\mu\varepsilon_{ij}(\boldsymbol{x}') + (\lambda\varepsilon_{kk}(\boldsymbol{x}') - \gamma\theta(\boldsymbol{x}'))\delta_{ij}, \tag{2}$$

and the strain tensor ε_{ij} at any two adjacent points $\boldsymbol{x}'$ and $\boldsymbol{x}$, defined by

$$\varepsilon_{ij}(\boldsymbol{x}') = 0.5\left(\frac{\partial u_i(\boldsymbol{x}')}{\partial x_j'} + \frac{\partial u_j(\boldsymbol{x}')}{\partial x_i'}\right) \tag{3}$$

In these equations, $\gamma = \frac{\alpha_t E}{(1-2\nu)} = \alpha_T E$, ν represents Poisson's ratio, E is Young's modulus, α_t is the linear thermal expansion, u_i is the components of the displacement, δ_{ij} refers to the function of Kronecker's delta, $\theta = T - T_0$ is the temperature change and T_0 is the environmental temperature. The Lamé's constants λ and μ can be expressed as $\lambda = E\nu/(1+\nu)(1-2\nu)$ and $\mu = E/2(1+\nu)$.

Also, $K_1(|\boldsymbol{x},\boldsymbol{x}'|,\xi)$ is a positive scalar kernel function, $\boldsymbol{x}-\boldsymbol{x}'$ is the Euclidean distance, $\xi = e_0 a/l_0$ is the nonlocal scale parameter, a is the internal characteristic length, l_0 is the external characteristic length and e_0 is a parameter that determined experimentally and called the material-dependent constant. When the kernel K_1 is chosen as [56,57]:

$$K_1(|\boldsymbol{x},\boldsymbol{x}'|,\xi) = \frac{1}{2\pi\xi^2 l^2} K_0\left(\frac{\boldsymbol{x}-\boldsymbol{x}'}{\xi l}\right), \tag{4}$$

where K_0 is the modified Bessel function, Eq. (1) may be simplified as [56,57]:

$$\left(1-\xi^2\nabla^2\right)\tau_{ij}(\boldsymbol{x}) = \sigma_{ij}(\boldsymbol{x}'), \tag{5}$$

which takes into account the size effect on the response of nanostructures.

Using Eq. (3) in (4), the following nonlocal constitutive stress-strain equation is obtained

$$\left(1-\xi^2\nabla^2\right)\tau_{ij} = C_{ijkl}\varepsilon_{kl} - \gamma_{ij}\theta \tag{6}$$

According to the modified couple stress (MCS) model, the strain energy density function is formed by multiplying the Cauchy stress tensor by the Cauchy strain tensor and conjugating the couple stress tensor with the curvature tensor. The following are the definitions for these tensors [58,59]:

$$2\varepsilon_{kl} = \frac{\partial u_k}{\partial x_l} + \frac{\partial u_l}{\partial x_k}, \tag{7}$$

$$m_{kl} = 2l^2\mu\chi_{kl} = 2\alpha\chi_{kl}, \tag{8}$$

$$2\chi_{kl} = \frac{\partial \omega_k}{\partial x_l} + \frac{\partial \omega_l}{\partial x_k}, \tag{9}$$

$$2\omega_k = \varepsilon_{kji}u_{i,j}. \tag{10}$$

where m_{kl} represents the local deviatoric portion of the couple stress (CS) tensor, l symbolizes the length scale parameter and χ_{kl} denotes the homogeneous part of the curvature tensor and ω_k indicates the rotation vector.

Tzou [47–49] has proposed a new generalized dual-phase-lag thermoelastic model. According to this model, the heat conduction equation that includes two-phase lags (τ_θ and τ_q) is given by

$$\left(1+\tau_{\theta}\frac{\partial}{\partial t}\right)\left(K\theta_{,i}\right)_{,i}=\left(1+\tau_{q}\frac{\partial}{\partial t}+\frac{1}{2}\tau_{q}^{2}\frac{\partial^{2}}{\partial t^{2}}\right)\left(\rho C_{E}\frac{\partial\theta}{\partial t}+\gamma T_{0}\frac{\partial e}{\partial t}-\rho Q\right), \tag{12}$$

where Q is the heat source K implies the thermal conductivity, C_E denotes the specific heat for each unit mass and ρ is the material density, and $e = \text{div } \vec{u}$ is the volumetric strain.

3. Problem formulation

The components of the system under consideration are a rotating nanobeam with length L, thickness h, and width b, bending stiffness EI, $I = bh^3/12$, deflection w and internal cross-sectional area $A = bh$, as illustrated in Fig. 1. The displacements of any point (x,y,z) on the neutral axis may be calculated using the Euler–Bernoulli beam theory (EBBT) as follows

$$u=-z\frac{\partial w}{\partial x}, v=0, w=w(x,t). \tag{13}$$

The components of the rotation vector ω_k can also be written as:

$$\omega_y=-\frac{\partial w}{\partial x}, \omega_x=\omega_z=0. \tag{14}$$

Introducing Eq. (14) into Eq. (9), we get

$$2\chi_{xy}=-\frac{\partial^2 w}{\partial x^2}, \chi_{xz}=\chi_{zx}=\chi_{zy}=\chi_{yz}=0. \tag{15}$$

The local constitutive relationships along the x-axis have only non-zero components when planar stress conditions are considered. These results can be determined by

$$\sigma_x=-E\left(z\frac{\partial^2 w}{\partial x^2}+\alpha_T\theta\right), m_{xy}=-l^2\mu\frac{\partial^2 w}{\partial x^2} \tag{16}$$

The nonlocal constituent equations, as suggested by the Eringen theory [6], can be expressed as [59]:

$$\tau_{xx}-\xi^2\frac{\partial^2\tau_{xx}}{\partial x^2}=\sigma_x=-E\left(z\frac{\partial^2 w}{\partial x^2}+\alpha_T\theta\right), \tag{17}$$

$$\mu_{xy}-\xi^2\frac{\partial^2\mu_{xy}}{\partial x^2}=m_{xy}=-l^2\mu\frac{\partial^2 w}{\partial x^2}, \tag{18}$$

where $\alpha_T = \alpha_t/(1-2\nu)$, τ_{xx} and μ_{xy} denote respectively, the nonlocal thermal and couple stresses.

The stress M_σ and stress M_m resultants can be given according to Euler–Bernoulli nanobeam and MCS theories as [59].

$$\begin{aligned} M_\sigma &= b\int_{-h/2}^{h/2} z\sigma_x \mathrm{d}z, \\ M_m &= b\int_{-h/2}^{h/2} \mu_{xy}\mathrm{d}z. \end{aligned} \tag{19}$$

The resulting total non-local bending moment M of the nanobeam may be determined using the following relationship [59].

$$M=M_\sigma+M_m \tag{20}$$

If we define the thermal moment M_T as

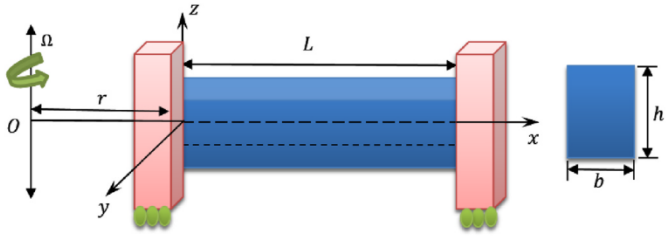

Fig. 1. Schematic chart for the nanobeam.

$$M_T = \frac{12}{h^3}\int_{-h/2}^{h/2} \theta(x,z,t) z \mathrm{d}z, \tag{21}$$

and using equations 17–20, bending moment M satisfies the following equation

$$M(x,t) - \xi \frac{\partial^2 M(x,t)}{\partial x^2} = -EI\left(\frac{\partial^2 w}{\partial x^2} + \alpha_T M_T\right) - I^2 \mu A \frac{\partial^2 w}{\partial x^2} \tag{22}$$

The motion equation for nanobeams under transverse vibration may be expressed as

$$\frac{\partial^2 M}{\partial x^2} = \rho A \frac{\partial^2 w}{\partial t^2} \tag{23}$$

We assume the considered nanobeam rotates with constant rotational velocity Ω along an axis parallel to the z-axis, centered at a short distance r (hub) from the nanobeam's initial edge. Rotation introduces the centrifugal tensional force $R(x)$. The equation of transverse motion (23) of the rotating nanobeams, in this situation, may be written as [32,33].

$$\frac{\partial^2 M}{\partial x^2} = \rho A \frac{\partial^2 w}{\partial t^2} - \frac{\partial}{\partial x}\left(R(x)\frac{\partial w}{\partial x}\right) \tag{24}$$

When the angular velocity Ω is zero (no rotation), then the centrifugal tension force $R(x)$ vanishes.
The centrifugal stiffening axial force $R(x)$ can be determined at a given distance x from the origin of rotation (see Fig. 1) as [32,33].

$$R(x) = \int_x^L \rho A \Omega^2 (r+\phi) d\phi \tag{25}$$

After integration, then Eq. (25) can be simplified as

$$R(x) = \frac{\rho A \Omega^2}{2}\left[2r(L-x) + L^2 - x^2\right] \tag{26}$$

Equations (22) and (24) may be used to calculate the bending moment $M(x,t)$ as

$$M(x,t) = \xi^2\left(\rho A \frac{\partial^2 w}{\partial t^2} - \frac{\partial}{\partial x}\left(R(x)\frac{\partial w}{\partial x}\right)\right) - EI\left(\left(1 + \frac{6l^2}{h^2(1+\nu)}\right)\frac{\partial^2 w}{\partial x^2} + \alpha_T M_T\right) \tag{27}$$

Motion equation (24) if the moment M is withdrawn from Eqs. (24) and (27) can be expressed as

$$\left[\left(1 + \frac{6l^2}{h^2(1+\nu)}\right)\frac{\partial^4}{\partial x^4} + \frac{\rho A}{EI}\frac{\partial^2}{\partial t^2}\left(1 - \xi\frac{\partial^2}{\partial x^2}\right)\right] w - \left(1 - \xi^2\frac{\partial^2}{\partial x^2}\right)\left[\frac{\partial}{\partial x}\left(R(x)\frac{\partial w}{\partial x}\right)\right] + \alpha_T \frac{\partial^2 M_T}{\partial x^2} = 0 \tag{28}$$

The modified heat conduction equation (12) is given in the absence of heat sources $(Q = 0)$ as

$$\left(1 + \tau_\theta \frac{\partial}{\partial t}\right)\left[\frac{\partial}{\partial x}\left(K(\theta)\frac{\partial \theta}{\partial x}\right) + \frac{\partial}{\partial z}\left(K(\theta)\frac{\partial \theta}{\partial z}\right)\right] = \left(1 + \tau_q \frac{\partial}{\partial t} + \frac{\tau_q^2}{2}\frac{\partial^2}{\partial t^2}\right)\frac{\partial}{\partial t}\left(\rho C_E(\theta)\theta - \gamma T_0 z \frac{\partial^2 w}{\partial x^2}\right) \tag{29}$$

One of the goals of this study is to explain the influence of thermal conductivity's temperature dependence while keeping the other parameters constant. Thermoelastic materials, according to the formula, exhibit temperature-dependent characteristics [22,60].

$$\eta = \frac{K(\theta)}{\rho C_E(\theta)}, \tag{30}$$

where η is the thermal diffusivity of the material. The following mapping (Kirchhoff's transform) is used to transform nonlinear heat equation (29) into linear ones [22].

$$\psi = \int_0^\theta \frac{K(\vartheta)}{K_0} \mathrm{d}\vartheta, \tag{31}$$

where K_0 indicates the thermal conductivity that is temperature independent. Equation (29) can be reduced to a linear partial differential equation with the help of equation (31)

$$\left(1 + \tau_\theta \frac{\partial}{\partial t}\right)\left(\frac{\partial^2}{\partial x^2} + \frac{\partial^2}{\partial z^2}\right)\psi = \left(1 + \tau_q \frac{\partial}{\partial t} + \frac{1}{2}\tau_q^2 \frac{\partial^2}{\partial t^2}\right)\frac{\partial}{\partial t}\left(\frac{1}{\eta}\psi - \frac{\gamma T_0}{K_0} z \frac{\partial^2 w}{\partial x^2}\right) \tag{32}$$

We assume there is no heat movement between the nanobeam's top and bottom surfaces. This indicates that $\frac{\partial \theta}{\partial z} = \frac{\partial \psi}{\partial z} = 0$ at $z = \pm h/2$. Furthermore, we suppose that the functions ψ and θ vary in a sinusoidal manner in the thickness direction provided by

$$\left\{\begin{array}{c}\theta(x,z,t)\\ \psi(x,t,z)\end{array}\right\}=\left\{\begin{array}{c}\Theta(x,t)\\ \Psi(x,t)\end{array}\right\}\sin\left(\frac{\pi}{h}z\right) \tag{33}$$

Presenting Eq. (31) into Eqs. (22), (23) and (30), leads to

$$\left[S_1\frac{\partial^4}{\partial x^4}+\frac{\rho A}{EI}\frac{\partial^2}{\partial t^2}\left(1-\xi\frac{\partial^2}{\partial x^2}\right)\right]w-\frac{1}{EI}\left(1-\xi^2\frac{\partial^2}{\partial x^2}\right)\left[\frac{\partial}{\partial x}\left(R(x)\frac{\partial w}{\partial x}\right)\right]+\frac{24\alpha_T}{\pi^2 h}\frac{\partial^2\Psi}{\partial x^2}=0, \tag{34}$$

$$M(x,t)=\xi^2\left(\rho A\frac{\partial^2 w}{\partial t^2}-\frac{\partial}{\partial x}\left(R(x)\frac{\partial w}{\partial x}\right)\right)-EI\left(S_1\frac{\partial^2 w}{\partial x^2}+\frac{24\alpha_T}{\pi^2 h}\frac{\partial^2\Phi}{\partial x^2}\right). \tag{35}$$

Substituting Eq. (33) into Eq. (32) and integrating with respect to z from $-h/2$ to $-h/2$ and with, we get

$$\left(1+\tau_\theta\frac{\partial}{\partial t}\right)\left(\frac{\partial^2}{\partial x^2}-\frac{\pi^2}{h^2}\right)\Psi=\left(1+\tau_q\frac{\partial}{\partial t}+\frac{1}{2}\tau_q^2\frac{\partial^2}{\partial t^2}\right)\frac{\partial}{\partial t}\left(\frac{1}{k}\Psi-\frac{\gamma T_0\pi^2 h}{24K_0}\frac{\partial^2 w}{\partial x^2}\right), \tag{36}$$

where $S_1=\left(1+\frac{6I^2}{h^2(1+\nu)}\right)$.

The following non-dimensional variables are provided for convenience

$$\begin{aligned}&\{u',x',L',w',z',h',b',\xi'\}=\eta c\{u,x,L,w,z,h,b,\xi\},\ \{\Theta',\Psi'\}=\frac{1}{T_0}\{\Theta,\Psi\},\\&\left\{t',\tau_q',\tau_\theta'\right\}=\eta c^2\{t,\tau_q,\tau_\theta\},\quad M'=\frac{1}{\eta cEI}M,\ c^2=\frac{E}{\rho}.\end{aligned} \tag{37}$$

After introducing dimensionless quantities (37) in Eqs. 34–36, we can obtain

$$\left[S_1\frac{\partial^4}{\partial x^4}+\frac{12}{h^2}\frac{\partial^2}{\partial t^2}\left(1-\xi^2\frac{\partial^2}{\partial x^2}\right)\right]w-\left(1-\xi^2\frac{\partial^2}{\partial x^2}\right)\left[\frac{\partial}{\partial x}\left(R(x)\frac{\partial w}{\partial x}\right)\right]+\frac{24T_0\alpha_T}{\pi^2 h}\frac{\partial^2\Psi}{\partial x^2}=0, \tag{38}$$

$$\left(1+\tau_\theta\frac{\partial}{\partial t}\right)\left(\frac{\partial^2}{\partial x^2}-\frac{\pi^2}{h^2}\right)\Psi=\left(1+\tau_q\frac{\partial}{\partial t}+\frac{1}{2}\tau_q^2\frac{\partial^2}{\partial t^2}\right)\frac{\partial}{\partial t}\left(\Psi-\frac{\gamma\pi^2 h}{24K_0\eta}\frac{\partial^2 w}{\partial x^2}\right), \tag{39}$$

$$M(x,t)=\frac{12\xi}{h^2}\frac{\partial^2 w}{\partial t^2}-\xi^2\left[\frac{\partial}{\partial x}\left(R(x)\frac{\partial w}{\partial x}\right)\right]-\left(S_1\frac{\partial^2 w}{\partial x^2}+\frac{24T_0\alpha_T}{\pi^2 h}\Theta\right). \tag{40}$$

The primes are removed for convenience in Eqs. 38–40.

We assume that the nanobeam rotates at a constant rotational speed throughout this study and that the centrifugal tension force $R(x)$ is the maximum value [32,33]. Due to centrifugal stiffening at the root ($x=0$), the maximal axial force $R(x)$ has the following form [32].

$$R_{max}=\int_0^L\rho A\Omega^2(r+x)dx=\frac{1}{2}\rho A\Omega^2L(2r+L) \tag{41}$$

The motion equation (38) is therefore can be described as

$$\begin{aligned}\left[S_1\frac{\partial^4}{\partial x^4}+\frac{12}{h^2}\frac{\partial^2}{\partial t^2}\left(1-\xi^2\frac{\partial^2}{\partial x^2}\right)\right]w-\frac{6L\Omega^2(2r+L)}{h^2}\left(1-\xi^2\frac{\partial^2}{\partial x^2}\right)\frac{\partial^2 w}{\partial x^2}\\+\frac{24T_0\alpha_T}{\pi^2 h}\frac{\partial^2\Psi}{\partial x^2}=0\end{aligned} \tag{42}$$

The bending moment in Eq. (40) may also be defined as

$$M(x,t)=\frac{12\xi^2}{h^2}\frac{\partial^2 w}{\partial t^2}-\frac{6L\Omega^2\xi^2(2r+L)}{h^2}\frac{\partial^2 w}{\partial x^2}-\left(S_1\frac{\partial^2 w}{\partial x^2}+\frac{24T_0\alpha_T}{\pi^2 h}\Theta\right) \tag{43}$$

4. Laplace transform technique

The Laplace transform formula defines the Laplace transform of any function $g(x,t)$, which is represented by $\Im\{g(x,t)\}$ or $G(x,s)$ can be expressed as

$$\Im\{g(x,t)\}=\int_0^\infty g(x,t)e^{-st}dt,\quad s>0, \tag{44}$$

Using Laplace technique under the initial conditions

$$\Psi(x,0)=\frac{\partial\Psi(x,0)}{\partial t}=0,\quad w(x,0)=\frac{\partial w(x,0)}{\partial t}=0,$$

equations (39), (42) and (43) are converted as

$$\left[\left(S_1+A_1\xi^2\right)\frac{\mathrm{d}^4}{\mathrm{d}x^4}-\left(A_0\xi^2+A_1\right)\frac{\mathrm{d}^2}{\mathrm{d}x^2}+A_0\right]\overline{w}=-A_2\frac{\mathrm{d}^2\overline{\Psi}}{\mathrm{d}x^2} \tag{45}$$

$$B_1\frac{\mathrm{d}^2\overline{w}}{\mathrm{d}x^2}=-\left(\frac{\mathrm{d}^2}{\mathrm{d}x^2}-B_2\right)\overline{\Psi}, \tag{46}$$

$$M(x,t)=\left[\xi^2A_0-\left(S_1+A_1\xi^2\right)\frac{\mathrm{d}^2}{\mathrm{d}x^2}\right]\overline{w}-A_2\overline{\Theta} \tag{47}$$

where

$$\begin{aligned}&A_1=\frac{6L\Omega^2(2r+L)}{h^2},A_2=\frac{24T_0\alpha_T}{\pi^2h},A_3=\frac{\gamma\pi^2h}{24K\eta},A_4=\frac{s\left(1+\tau_q\mathrm{s}+s^2\tau_q^2\Big/2\right)}{(1+\tau_\theta s)},\\&B_1=A_3A_4,B_2=\frac{\pi^2}{h^2}+A_4,A_0=\frac{12s^2}{h^2}.\end{aligned} \tag{48}$$

5. Application

In the previous section, the problem was solved for any selectable boundary conditions in the Laplace transform domain. As an application to the suggested problem and to set the undetermined parameters $C_j,(j=1,2..,6)$, we will impose some boundary conditions on the nanobeam. In this work, we consider that both ends of the microbeam are simply supported. In addition, we assume that the first end is thermally loaded while the last edge is insulated. In this case, we find that the nanobeam satisfies the following boundary conditions:

$$w(x,t)|_{x=0,L}=0,\left.\frac{\partial^2w(x,t)}{\partial x^2}\right|_{x=0,L}=0. \tag{49}$$

At the first end $x=0$, the nanobeam loaded thermally by a sinusoidal heat pulse as

$$\theta(x,0)=L(t)=\Theta_0\sin\left(\frac{\pi t}{\omega}\right),0\le t\le\omega, \tag{50}$$

where Θ_0 is a constant and ω is the thermal vibration time size. Several width pulses each half-cycle are utilized in sinusoidal pulse width variation. Various pulsed thermal shock drivers are used in a variety of industrial applications that require improved performance.

Additionally, the temperature at the second end satisfies the boundary listed below

$$\frac{\partial\theta}{\partial x}=0\quad\text{on}\quad x=L. \tag{51}$$

It was taken into account that the thermal conductivity in the present work is a linear function of temperature changes and is given by [35].

$$K(\theta)=K_0(1+K_1\theta),K_1\le0. \tag{52}$$

By using the mapping in Eq. (17), one gets

$$\psi=\theta+\frac{K_1\theta^2}{2}. \tag{53}$$

Presenting Eq. (17) into equations (50) and (51), then we have

$$\Psi(0,t)=L(t)+\frac{1}{2}K_1[L(t)]^2, \tag{54}$$

$$\frac{\partial\Psi(L,t)}{\partial x}=0. \tag{55}$$

The boundary conditions (50), (54) and (55) may be entered in the transformation domain as

$$\overline{w}(x,s)|_{x=0,L}=0,\left.\frac{\mathrm{d}^2\overline{w}(x,s)}{\mathrm{d}x^2}\right|_{x=0,L}, \tag{56}$$

$$\overline{\Psi}(x,s)|_{x=0}=\frac{\omega\pi\Theta_0}{\pi^2+s^2\omega^2}+\frac{K_1\pi^2\Theta_0^2}{4\pi^2 s+s^3\omega^2}=\overline{G}(s), \tag{57}$$

$$\left.\frac{\mathrm{d}\overline{\Psi}}{\mathrm{d}x}\right|_{x=L}=0. \tag{58}$$

6. State-space approach mathematical technique

The differential and algebraic equations can be represented in matrix form if the dynamical system is linear, time constant and finite dimensional [61]. The state-space method is characterized by a large general system theory algebra, which allows the use of Kronecker vector-matrix structures. With or without modification, these structures can be effectively used to research systems [62]. The state-space technique facilitates the application of the advanced model of the control process to the issues of elastic and thermoelastic theories. In the field of thermoelasticity, Bahar and Hetnarski [54] were pioneers of the state-space method.

Now, we will introduce a new function $\overline{\Phi}$, which fulfills the following relation

$$\overline{\Phi}=\frac{\mathrm{d}^2\overline{w}}{\mathrm{d}x^2} \tag{59}$$

Eqs. (45) and (46) can be written as follows after using Eq. (59)

$$\frac{\mathrm{d}^2\overline{\Psi}}{\mathrm{d}x^2}=B_1\overline{\Psi}-B_2\overline{\Phi}, \tag{60}$$

$$\frac{\mathrm{d}^2\overline{\Phi}}{\mathrm{d}x^2}=-B_3\overline{w}-B_4\overline{\Psi}+B_5\overline{\Phi}, \tag{61}$$

where

$$\begin{aligned} &B_3=A_6, B_4=B_1A_7B_5=A_5+B_2A_7,\\ &A_5=\frac{A_1+A_0\xi^2}{S_1+A_1\xi^2}, A_6=\frac{A_0}{S_1+A_1\xi^2}, A_7=\frac{A_2}{S_1+A_1\xi^2}. \end{aligned} \tag{62}$$

In matrix form, equations 59–61 may be written as

$$\frac{\mathrm{d}\overline{\boldsymbol{V}}(x,s)}{\mathrm{d}x}=\boldsymbol{A}(s)\overline{\boldsymbol{V}}(x,s), \tag{63}$$

where

$$\overline{\boldsymbol{V}}(x,s)=\begin{bmatrix}\overline{w}\\ \overline{\Psi}\\ \overline{\Phi}\\ \overline{w}'\\ \overline{\Psi}'\\ \overline{\Phi}'\end{bmatrix} \text{ and } \boldsymbol{A}(s)=\begin{bmatrix}0 & 0 & 0 & 1 & 0 & 0\\ 0 & 0 & 0 & 0 & 1 & 0\\ 0 & 0 & 0 & 0 & 0 & 1\\ 0 & 0 & 1 & 0 & 0 & 0\\ 0 & B_1 & -B_2 & 0 & 0 & 0\\ -B_3 & -B_4 & B_5 & 0 & 0 & 0\end{bmatrix}. \tag{64}$$

The transformed temperature and displacement, as well as the gradients, form the state vector $\overline{\boldsymbol{V}}(x,s)$ in the transformation domain. The exponential matrix can be used to integrate the differential equation. (63) to get

$$\overline{\boldsymbol{V}}(x,s)=\exp[\boldsymbol{A}(s).x]\overline{\boldsymbol{V}}(0,s), \tag{65}$$

where the $\exp[\boldsymbol{A}(s).x]$ is the exponential transfer matrix and the vector $\overline{\boldsymbol{V}}(0,s)$ is given by

$$\overline{\boldsymbol{V}}(0,s)=[\overline{w}(0,s)\quad \overline{\Psi}(0,s)\quad \overline{\Phi}(0,s)\quad \overline{w}'(0,s)\quad \overline{\Psi}'(0,s)\quad \overline{\Phi}'(0,s)]^{Tr} \tag{66}$$

Due to the Cayley-Hamilton theorem, the matrix exponential's Taylor-series expansion stops with the term containing the cube of the matrix $\boldsymbol{A}(s)$, allowing it to be determined explicitly [58]. This is because the characteristic equation that corresponds to the matrix $\boldsymbol{A}(s)$ in Eq. (4) is provided by

$$m^6-Am^4+Bm^2-C=0, \tag{67}$$

Where the parameters m are the root of characteristic Eq. (67) and satisfy the relations

$$m_1^2+m_2^2+m_3^2=A, m_1^2m_2^2+m_2^2m_3^2+m_3^2m_1^2=B, m_1^2m_2^2m_3^2=C. \tag{68}$$

where

$$\begin{aligned} &A=A_7+B_2+A_7B_1, B=A_6+A_5B_2, C=A_6B_2\\ &A_5=\frac{A_1+A_0\xi^2}{S_1+A_1\xi^2}, A_6=\frac{A_0}{S_1+A_1\xi^2}, A_7=\frac{A_2}{S_1+A_1\xi^2}. \end{aligned} \tag{69}$$

In the matrix sense, the Cayley-Hamilton theorem says that the matrix $A(s)$ satisfies its own characteristic equation. It follows from this that

$$\boldsymbol{A}^6-A\boldsymbol{A}^4+B\boldsymbol{A}^2-C\boldsymbol{I}=0, \tag{70}$$

The McLaurin series expansion for the matrix $\exp[A(s).x]$ may be written as

$$\exp[A(s).x]=\sum_{n=0}^{\infty}\left(\frac{(\exp[A(s).x])^n}{n!}\right). \tag{71}$$

Equation (7) demonstrates that $\boldsymbol{A}^5$ and all higher powers of $\boldsymbol{A}$ may be represented in terms of $\boldsymbol{A}^4$, $\boldsymbol{A}^3$, $\boldsymbol{A}^2$, $\boldsymbol{A}$ and the six-order unit matrix $\boldsymbol{I}$. The exponential matrix $\exp[A(s).x]$ may now be expressed as

$$\exp[\boldsymbol{A}(s).x]=a_0\boldsymbol{I}+a_1\boldsymbol{A}+a_2\boldsymbol{A}^2+a_3\boldsymbol{A}^3+a_4\boldsymbol{A}^4+a_5\boldsymbol{A}^5 \tag{72}$$

Where coefficients a_j, $(j=0,1,\ldots..,5)$ are functions of the distance x and the parameter, respectively. By replacing the matrix $\boldsymbol{A}$ with its characteristic roots $\pm m_1$, $\pm m_2$ and $\pm m_3$ the scalar coefficients of Equation (72) are now calculated. Then, we have the following system of equations:

$$\begin{aligned} \exp[\pm m_i.x]&=a_0+a_1m_i+a_2{m_i}^2+a_3{m_i}^3+a_4{m_i}^4+a_5{m_i}^5, i=1,2,3,\\ &=L(x,s)=\left[L_{ij}(x,s)\right], i,j=1,2,\ldots.,6. \end{aligned} \tag{73}$$

Appendix (I) contains the solution to the system equation (73) and Appendix (II) contains the coefficients of the matrix $[L_{ij}(x,s)]$. Then, the solutions are then given by [63].

$$\begin{bmatrix} \overline{w}\\ \overline{\Psi}\\ \overline{\Phi}\\ \overline{w}'\\ \overline{\Psi}'\\ \overline{\Phi}' \end{bmatrix}=\begin{bmatrix} L_{11} & L_{12} & L_{13} & L_{14} & L_{15} & L_{16}\\ L_{21} & L_{22} & L_{23} & L_{24} & L_{25} & L_{26}\\ L_{31} & L_{32} & L_{33} & L_{34} & L_{35} & L_{36}\\ L_{41} & L_{42} & L_{43} & L_{44} & L_{45} & L_{46}\\ L_{51} & L_{52} & L_{53} & L_{54} & L_{55} & L_{56}\\ L_{61} & L_{62} & L_{63} & L_{64} & L_{65} & L_{66} \end{bmatrix}\begin{bmatrix} \overline{w}(0,s)\\ \overline{\Psi}(0,s)\\ \overline{\Phi}(0,s)\\ \overline{w}'(0,s)\\ \overline{\Psi}'(0,s)\\ \overline{\Phi}'(0,s) \end{bmatrix} \tag{74}$$

After performing some complex mathematical operations and using the **Mathematica** software in the calculations, we find that the final solutions in the transformed field are as follows

$$\begin{aligned} \overline{w}(x,s)=&\frac{G(s)\left(B_1-m_1^2\right)\left(B_1-m_2^2\right)\left(B_1-m_3^2\right)}{B_1B_2}\left[\frac{\sinh(m_1(L-x))}{\left(m_1^2-m_2^2\right)\left(m_1^2-m_3^2\right)\sinh(m_1L)}\right.\\ &\left.+\frac{\sinh(m_2(L-x))}{\left(m_2^2-m_1^2\right)\left(m_2^2-m_3^2\right)\sinh(m_2L)}+\frac{\sinh(m_3(L-x))}{\left(m_3^2-m_2^2\right)\left(m_3^2-m_1^2\right)\sinh(m_3L)}\right], \end{aligned} \tag{75}$$

$$\begin{aligned} \overline{\Psi}(x,z,s)=&-\frac{G(s)\left(B_1-m_1^2\right)\left(B_1-m_2^2\right)\left(B_1-m_3^2\right)\sin(\pi z/h)}{B_1}\left[\frac{m_1^2\sinh(m_1(L-x))}{\left(m_1^2-B_1\right)\left(m_1^2-m_2^2\right)\left(m_1^2-m_3^2\right)\sinh(m_1L)}\right.\\ &\left.+\frac{m_2^2\sinh(m_2(L-x))}{\left(m_2^2-B_1\right)\left(m_2^2-m_3^2\right)\left(m_2^2-m_1^2\right)\sinh(m_2L)}+\frac{m_1^2\sinh(m_1(L-x))}{\left(m_3^2-B_1\right)\left(m_3^2-m_1^2\right)\left(m_3^2-m_2^2\right)\sinh(m_3L)}\right]. \end{aligned} \tag{76}$$

Also, the displacement after using Eq. (68) can be written as

$$\begin{aligned} \overline{u}(x,z,s)=&\frac{zG(s)\left(B_1-m_1^2\right)\left(B_1-m_2^2\right)\left(B_1-m_3^2\right)}{B_1B_2}\left[\frac{m_1\cosh(m_1(L-x))}{\left(m_1^2-m_2^2\right)\left(m_1^2-m_3^2\right)\sinh(m_1L)}\right.\\ &\left.+\frac{m_2\cosh(m_2(L-x))}{\left(m_2^2-m_1^2\right)\left(m_2^2-m_3^2\right)\sinh(m_2L)}+\frac{m_3\cosh(m_3(L-x))}{\left(m_3^2-m_2^2\right)\left(m_3^2-m_1^2\right)\sinh(m_3L)}\right]. \end{aligned} \tag{77}$$

Finally, the temperature solution $\overline{\theta}$ in the transformed domain may be obtained by solving Eq (53)

$$\overline{\theta}=\frac{-1+\sqrt{1+2K_0\overline{\Psi}}}{K_1}, \quad 1+2K_0\overline{\Psi}\geq 0. \tag{78}$$

7. Laplace transform inversion

There are many numerical algorithms in the literature, each with its own set of applications and suitability for a particular type of function. The Fourier series expansion, as well as the Honig and Hirdes technique [64] (called a fast-Fourier transform (FFT) method), will be briefly introduced in this paper. The Bromwich contour inversion integral, which can be written as an integral of a real-valued function of a real variable selecting a given contour, is the basis for this approach. In this method, all functions $\bar{g}(x,s)$ in the Laplace field can be converted to the time field $\bar{g}(x,s)$ by making use of the relation

$$g(x,t)=\frac{2e^{ct}}{t_1}\left\{\frac{1}{2}\,\mathrm{Re}[\bar{g}(x,c)]+\mathrm{Re}\left[\sum_{n=1}^{N}\bar{g}\left(x,c+\frac{in\pi}{t_1}\right)\cos\left(\frac{n\pi t}{t_1}\right)\right]\right\}, \tag{79}$$

where the parameter t_1 denotes the time interval while Re stands for the real part of the complex function. By summing a specific number N, Eq. (80) can now be calculated numerically. As a result, c and N are parameters that must be modified to improve accuracy. This approach has been proven to be very accurate based on previous experience and literature. The parameter may be selected as

$$c=\beta-\frac{ln(Err)}{2t_1}, \tag{80}$$

where Err is the error tolerance, β is the real part of the leading pole of the function $\bar{g}(x,s)$ [65]. In addition, several numerical investigations have demonstrated that parameter c fulfills $0<ct<5$ for faster convergence [66].

8. Results and discussion

In this work, numerical findings are provided by focusing on the parameters and physical constants in SI units, which are used in the formulations of the physical variables under consideration, and by using silicon as the material. The following values of important parameters were used for this purpose [37,38]:

$$E=169\ \mathrm{GPa},\quad \rho=2330\frac{\mathrm{kg}}{\mathrm{m}^3},\quad C_E=713\frac{\mathrm{J}}{\mathrm{kg\ K}},$$
$$\alpha_T=2.59\times10^{-9}\frac{1}{\mathrm{K}},\ \nu=0.22,\ T_0=293\ \mathrm{K},\ K=156\frac{\mathrm{W}}{\mathrm{mK}},$$
$$L=100\mathrm{nm},\ h=10\mathrm{nm},\ b=5\ \mathrm{nm},\quad l=4\mathrm{nm}.$$

We assume that the non-dimensional parameters L,h,b and l satisfy the relations $L/h=10$, $b/h=0.5$ and $h/l=2.5$ unless otherwise indicated.

In order to investigate their effect, we divided graphical representations of several features on the investigated thermophysical fields into three groups: size-dependent effects (ξ and l), variation of thermal conductivity (K_1), and angular velocity of rotation (Ω). The impact of various nonlocal parameter ξ and the size-dependent factor l has been studied in the first category (see Figs. 2–5). Figs. 6–9 in the second category depicted the impacts of angular rotational velocity Ω. At $t=0.1$s, all of the categories are shown.

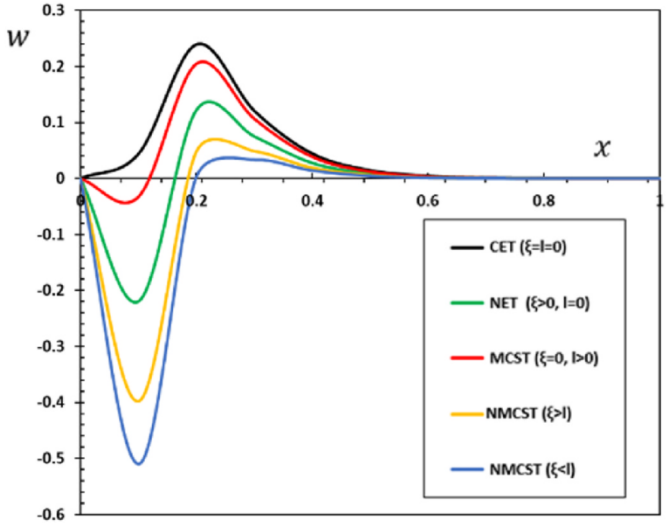

Fig. 2. The distribution of deflection w via local and nonlocal beam theories.

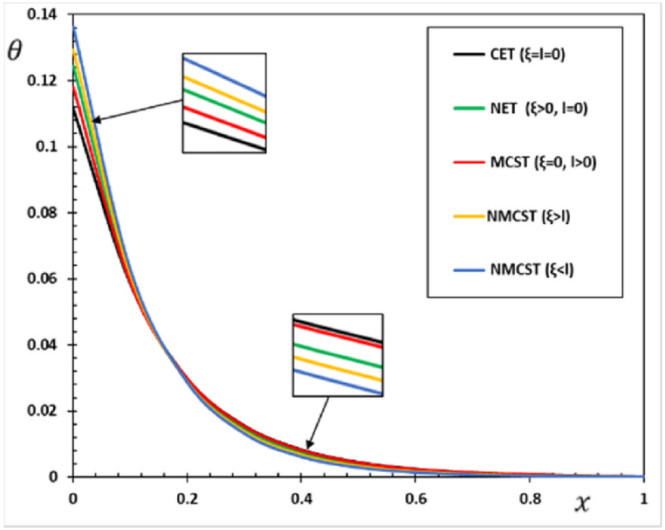

Fig. 3. The distribution of temperature θ via local and nonlocal beam theories.

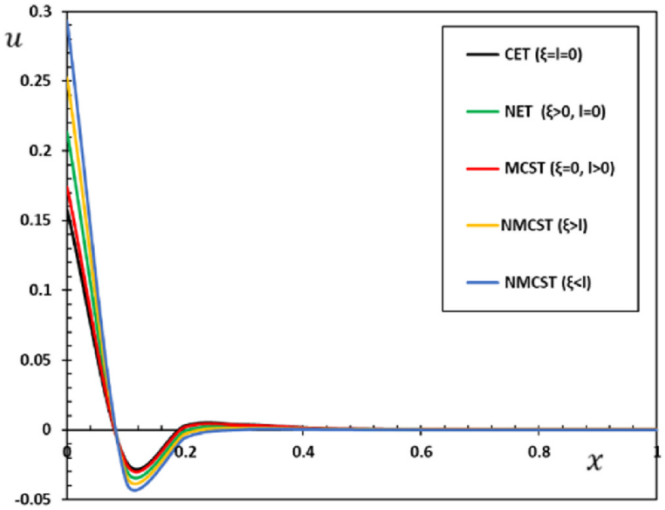

Fig. 4. The distribution of displacement u via local and nonlocal beam theories.

8.1. *Effect of nonlocal and material length scale coefficients*

When the cantilever thickness reaches the nanoscale, Sadeghian et al. [67] experimentally demonstrated that size-dependent mechanical characteristics of the silicon cantilever are important.

However, even for micro-scale beams, the size-dependent behavior of nanobeams is significant [68,69]. As a result, silicon micro-beam resonators, which are widely used in MEMS devices, are utilized to investigate the impacts of the length-scale parameters on the nanobeam response.

The importance of the scale coefficient in several field variables has been emphasized in the first illustration. For several materials, the nonlocal parameter ξ is measured experimentally; for a single-walled carbon nanotube, a cautious estimate of $\xi < 4(\text{nm})^2$ is suggested. The non-dimensional nonlocal parameter ξ is provided by $\xi = 10^{-6}$ in this investigation. A new parameter $\bar{\xi}$ ($\bar{\xi} = 10^6\xi$), will be introduced to further describe the influence of this parameter. For calculation purposes, the non-dimensional values $l = 0.01$, $K_1 = -0.3$, $\Omega = 0.3$, $\tau_q = 0.02$ and $\tau_\theta = 0.01$ are taken. The influence of the nano-scale (nonlocal parameter) effect on nanobeam vibration under thermal load is depicted using graphs 2–5.

We can note that, the nonlocal elasticity theory (NET) proposed by Eringen [6] can be derived if the parameter $l = 0$ and when $\xi = 0$, the modified couple stress theory (MCST) suggested by Yang et al. [14] can be obtained. The classical Euler–Bernoulli elastic beam theory (CET) can be derived if the parameters $\xi = l = 0$. The nonlocal modified couple stress theory (NMCST) can be discussed if $\xi, l >$

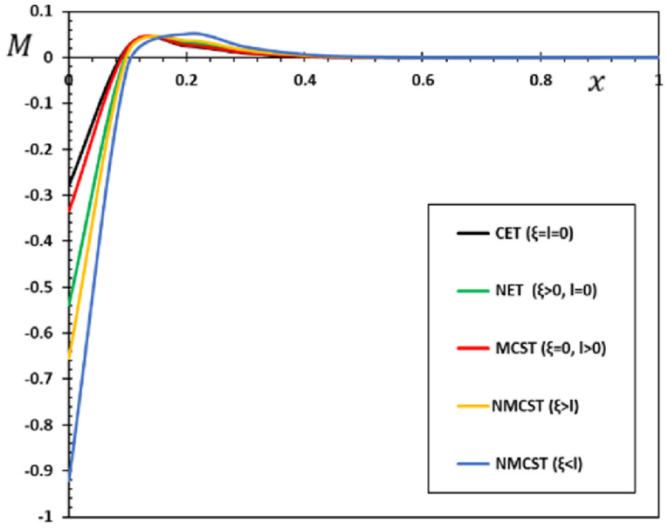

Fig. 5. The distribution of bending moment M via local and nonlocal beam theories.

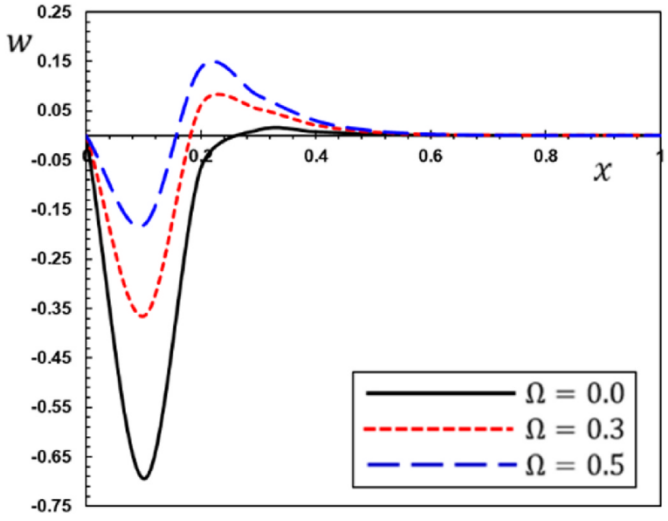

Fig. 6. The deflection w with different rotational speed Ω.

0. The differences between local and nonlocal theories are seen in Figs. 2–5.

There is no analytical or computational data on the vibration of thermoelastic rotating nanobeams and plates using a combination of modified couple stress theory and nonlocal elasticity theory, as well as generalized thermoelasticity with phase delays, to the best of the authors' knowledge. In this situation, there is also no experimental evidence to identify the length scale parameter or the nonlocal parameter. Usually only modified couple stress theory and non-local elasticity theory are used. As evidenced by the Figures, we can conclude that:

- Compared with previous studies as in Ref. [23], we found that there is a strong match between the results of the non-local modified couple stress theory and the data from the experimental study and molecular dynamics simulation.
- In contrast to the classical models, the nonlocal strain gradient elasticity model can show good agreement with experimental findings. In addition, when compared with the NET theory, the NMCST theory produces higher vibration frequencies for rotating nanobeams. This is owing to the couple stress theory inclusion of the length scale parameter, which causes the nanobeam structure to stiffen and harden.
- Figs. 2, 3, 4 and 5 show that the values of the studied variables in the case of NMCST, MCST and NET models are greater than those obtained using the traditional continuum theory (CET). In addition, the results of the NMCST model are lower than those of the non-local elastic (NET) model when the parameter l is set to a value greater than the parameter ξ.

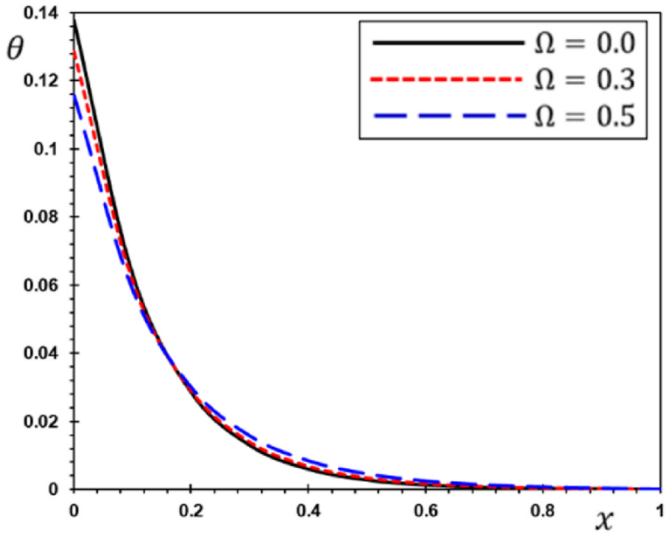

Fig. 7. The temperature θ with different rotational speed Ω.

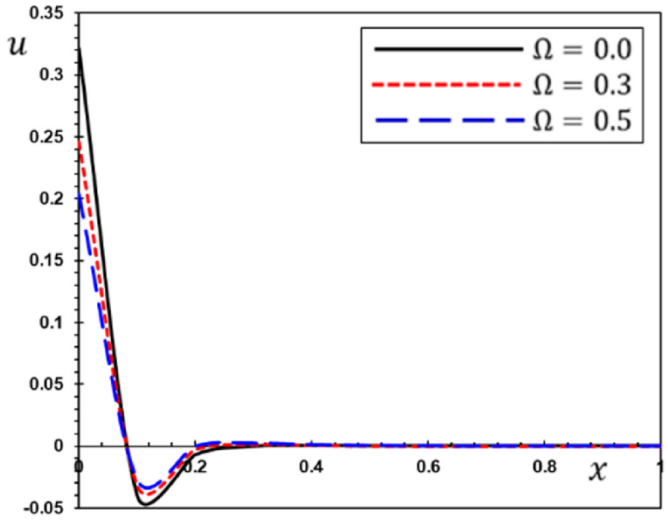

Fig. 8. The displacement u with different rotational speed Ω.

- The results indicate that the nanobeam has the effect of reducing the stiffness when the material length scale parameter is less than the non-local parameter and that the nanobeam has the effect of reducing the stiffness when the length scale parameter of the material is larger than the non-local parameter.
- Among the four theories, the presented NMCST model has the highest magnitude of non-dimensional field variables, whereas CET has the lowest.
- The modified couple stress concept and the nonlocal elasticity model both describe two distinct size-dependent micro/nano properties of materials. As a result, there is a technical need to examine both of these explanations of materials at the same time in order to build a more accurate size-dependent model for accurate evaluation of mechanical behavior of nanobeams with both stiffness-softening and stiffness-hardening effects.
- Lower non-local parameter values have a smaller difference between NMCST and MCST, while larger non-local parameter values have a greater difference. CET and NET are following this trend.
- Stress increases while strain decreases in Eringen's differential formulation when it comes to reducing results due to higher values of non-local parameters. As a result, the effect was softer. Thus the deflections are reduced by increasing the non-local parameter. The present results are in good agreement with those of Jena et al. [70].

The nonlocal effect dominates when the material length scale parameter l is smaller than the nonlocal parameter ξ, resulting in a

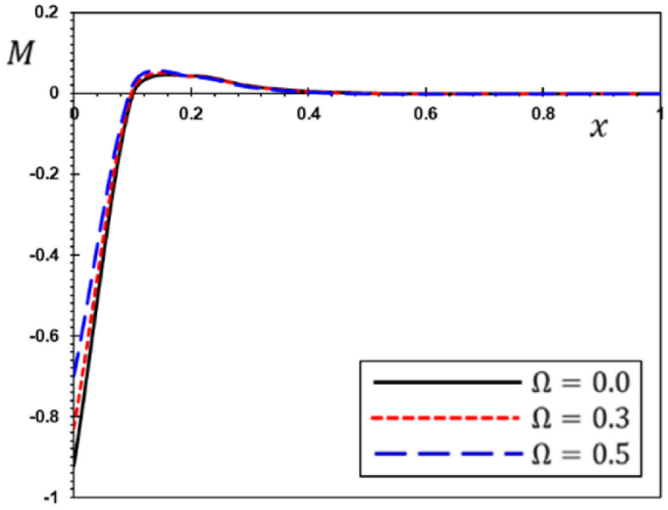

Fig. 9. The bending moment M with different rotational speed Ω.

stiffness-softening effect in the nanobeam, as can be seen in the pictures. The strain gradient effect takes priority when the nonlocal parameter ξ is larger than the material length scale parameter l, resulting in the nanobeam stiffening. In fact, for larger length scale parameters, the effect of nonlocal factors on dimensionless investigated field variables is more pronounced. As the length scale parameter of the spinning nanobeam increases, the softening impact of the nonlocal parameter becomes more noticeable. As a result, considering these two factors while modeling nanobeams is critical for proper analysis.

8.2. *The effect of the angular velocity of rotation*

In this subsection, a study is carried out to evaluate the effect of angular rotation speed Ω on the physical field variables. The discussion will be done when the values of the other effective parameters are constant. The difference in the fields tested for three different values of angular velocity ($\Omega = 0, 0.1, 0.3$) is illustrated in Figs. 6–9. In the absence of a rotation, which is a special situation in the present method, the rotation coefficient is zero ($\Omega = 0$). The vibration of the system is found to be strongly influenced by the rotational speed Ω.

The deflection w of the rotating nanobeam is affected by the change in the parameter of the angular rotation speed Ω, as shown in Fig. 6. This parameter has been shown to have a significant effect on the distribution of the deflection w and the variability in the results in the presence and absence of the rotation (due to the centrifugal force). As the angular velocity Ω rises, we observe a rise in the values of deviation w. These findings and behaviors are comparable to those reported in Refs. [41,42,71].

The temperature change θ in the nanobeams with distance x has been validated for several non-dimensional angular velocity Ω values. Fig. 7 depicts the possible causes of these differences. The influence of rotation Ω on temperature change is either minimal or non-existent, as seen in the graph. The findings and observations of the previous literature are consistent with the author's findings and observations, as evidenced by the equivalent findings in Refs. [41,42,72].

Fig. 8 shows the effect of the angular velocity Ω on the variance of the displacement u. We can see from the figure that the rotation speed Ω has a prominent effect on the curves depicting the displacement field. The figure also shows how increased rotation reduces the distribution of displacement at some intervals while increasing it at others. For the variable angular velocity values Ω, Fig. 9 shows how the bending moment M varies for a spinning nanobeam. The graph shows that rotation has a significant effect on the torque curves, with the moment amplitude increasing as the angular velocity values Ω decrease.

For innovative small electronics, a physical model of a rotating nanobeam is essential. One of the aims of this study was to explain how some nanoparticles, such as nanoturbines, interact with temperature changes and angular velocity changes, both of which provide valuable information [72]. The fundamental influence of rotation on the behavior of different physical distributions can also be inferred from the above facts and should be taken into account in manufacturing and design processes. Effective design of these rotating nano-machines requires a thorough understanding of their mechanical components, such as bending, vibration, and torsion. Due to the growing number of research demonstrating the potential of rotating nanostructures, this issue is expected to receive significant in the near future [73]. External kinetic and thermal variables, as well as intrinsic scale factors and their coupling effects, influence the dynamics of rotating thermal nanobeams.

9. Conclusions

In the present work, generalized thermoelasticity model with phase lag and Euler–Bernoulli beam theories were used to derive a new model to investigate thermoelastic vibration analysis of rotating nanobeams. The nanoscale system rotates about a fixed axis

perpendicular to the axial direction of the beam. The modified couple stress and Eringen's nonlocal elasticity models are used to the investigate the effects of material length scale and nonlocal parameters. The coefficient of thermal conductivity and specific heat of the nanobeam depend on the temperature change, which was taken into account.

The differential equations governing the vibrations of rotating nanobeams are solved using the Laplace transform method. The influence of nonlocal parameters, material length scale factor, thermal factors, rotation, and thermal conductivity variations on thermal and mechanical wave dispersion has been studied. It has been demonstrated to have a substantial impact on the thermoelastic vibrations of nano-spinning systems. Furthermore, the following significant outcomes are achieved:

- The difference between NMCST and MCST is less pronounced for lower non-local parameter values but becomes more clearer as non-local parameter values increase. This trend applies to both CET and the NET.
- The nonlocal modified couple stress elasticity model, in contrast to the conventional models, can show good agreement with experimental results. Deflections are reduced as the non-local parameter increases.
- The modified couple stress effect is a priority when the non-local parameter is greater than the length scale parameter of the material, which results in the annealing of the nanobeam.
- The fundamental influence of rotation on the behavior of the physical distributions may also be deduced from the data and should be considered in manufacturing and design processes.
- The parameter of thermal conductivity change affects the wave propagation rate in all the physical disciplines under investigation. The fluctuation of thermal conductivity and its relationship to temperature change have a significant impact on a variety of physical fields.
- Nanoscale materials may have temperature-dependent and size-dependent structures. This indicates that nonlocality behavior is strongly influenced by external temperature. The rotating nanobeam can act as a temperature-dependent structure as well.
- The obtained results indicated that the size-dependent effects on thermal vibrations of the nano-beam may be large, which confirms the importance of the size-dependent effects in nano-devices and system design.
- Since it deals with the optical and electrical characteristics of nanobeams, nanobeam research is crucial in nanotechnology. The current work may have implications for resonators, voltage surge sensors, frequency filters, accelerometers, and relay switches. This work will identify the various demands and requirements for the design and manufacture of environmentally sensitive resonators.

CRediT authorship contribution statement

Ahmed M.H. Yahya: Contribution to conception and design, Formal analysis, interpretation of data, Critically revising the article, Final approval of the version to be published. **Ahmed E. Abouelregal:** Contribution to conception and design, Study design, Methodology, Writing – original draft, Critically revising the article, Final approval of the version to be published. **K.M. Khalil:** Study design, Methodology, Acquisition and collation of data, Writing – original draft, Critically revising the article, Final approval of the version to be published. **Doaa Atta:** Acquisition and collation of data, Formal analysis, interpretation of data, Writing – original draft, Final approval of the version to be published.

Declaration of competing interest

The authors declare that they have no known competing financial interests or personal relationships that could have appeared to influence the work reported in this paper.

Acknowledgments

The authors extend their appreciation to the Deanship of Scientific Research at Jouf University for funding this work through research grant No. (DSR2021-03-0125). We would also like to extend our sincere thanks to the College of Science and Arts in Al-Qurayyat for its technical support.

References

[1] A. Babaei, M. Arabghahestani, Free vibration analysis of rotating beams based on the modified couple stress theory and coupled displacement field, Appl. Mech. 2 (2) (2021) 226–238.
[2] A. Babaei, A. Ghanbari, F. Vakili-Tahami, Size-dependent behavior of functionally graded micro-beams, based on the modified couple stress theory, Technology 3 (2015) 364–372.
[3] N.A. Fleck, G.M. Muller, M.F. Ashby, J.W. Hutchinson, Strain gradient plasticity: theory and experiment, Acta Metall. Mater. 42 (2) (1994) 475–487.
[4] A.C.M. Chong, D.C.C. Lam, Strain gradient plasticity effect in indentation hardness of polymers, J. Mater. Res. 14 (10) (1999) 4103–4110.
[5] S. Papargyri-Beskou, K.G. Tsepoura, D. Polyzos, D.E. Beskos, Bending and stability analysis of gradient elastic beams, Int. J. Solid Struct. 40 (2) (2003) 385–400.
[6] A.C. Eringen, On differential equations of nonlocal elasticity and solutions of screw dislocation and surface waves, J. Appl. Phys. 54 (9) (1983) 4703–4710.
[7] R.D. Mindlin, H.F. Tiersten, Effects of couple-stresses in linear elasticity, Arch. Ration. Mech. Anal. 11 (1) (1962) 415–448.
[8] R.A. Toupin, Elastic materials with couple-stresses, Arch. Ration. Mech. Anal. 11 (1) (1962) 385–414.
[9] W.T. Koiter, Couple-stresses in the theory of elasticityI and II, in: Proceedings of the Koninklijke Nederlandse Academie van Wetenschappen B: Physical Sciences, 67, 1964, pp. 17–44.
[10] A.C. Eringen, On differential equations of nonlocal elasticity and solutions of screw dislocation and surface waves, J. Appl. Phys. 54 (1983) 4703–4710.
[11] A.C. Eringen, D.G.B. Edelen, On nonlocal elasticity, Int. J. Eng. Sci. 10 (3) (1972) 233–248.

[12] Q. Wang, K.M. Liew, Application of nonlocal continuum mechanics to static analysis of micro- and nano-structures, Phys. Lett., A 363 (2007) 236–242.
[13] R.D. Mindlin, Micro-structure in linear elasticity, Arch. Ration. Mech. Anal. 16 (1) (1964) 51–78.
[14] F. Yang, A.C.M. Chong, D.C.C. Lam, P. Tong, Couple stress based strain gradient theory for elasticity, Int. J. Solid Struct. 39 (10) (2002) 2731–2743.
[15] A.R. Hadjesfandiari, G.F. Dargush, Evolution of generalized couple-stress continuum theories: a critical analysis, 2014 arXiv preprint arXiv:1501.03112.
[16] A.R. Hadjesfandiari, G.F. Dargush, Foundations of Consistent Couple Stress Theory, arXiv preprint arXiv:1509.06299, 2015.
[17] A.R. Hadjesfandiari, G.F. Dargush, Couple stress theories: theoretical underpinnings and practical aspects from a new energy perspective, 2016 arXiv preprint arXiv:1611.10249.
[18] S. Yin, Y. Deng, G. Zhang, T. Yu, S. Gu, A new isogeometric Timoshenko beam model incorporating microstructures and surface energy effects, Math. Mech. Solid 25 (2020) 2005–2022.
[19] A. Babaei, A. Rahmani, I. Ahmadi, Transverse vibration analysis of nonlocal beams with various slenderness ratios, undergoing thermal stress, Arch. Mech. Eng. 66 (2019) 5–24.
[20] M. Shahrokhi, E. Jomehzadeh, M. Rezaeizadeh, Size-dependent Green's function for bending of circular micro plates under eccentric load, J. Solid Mech. 11 (1) (2019) 14–25.
[21] D. Soltani, M.A. Khorshidi, H.M. Sedighi, Higher order and scale-dependent micro-inertia effect on the longitudinal dispersion based on the modified couple stress theory, J. Comput. Design Eng. 8 (1) (2021) 189–194.
[22] A. Duygu, Free vibrations of nanobeams under non-ideal supports based on modified couple stress theory, Z. Naturforsch. 76 (5) (2021) 427–434.
[23] A. Rahmani, S. Faroughi, M.I. Friswell, A. Babaei, Eringen's nonlocal and modified couple stress theories applied to vibrating rotating nanobeams with temperature effects, Mech. Adv. Mater. Struct. (2021), https://doi.org/10.1080/15376494.2021.1939468.
[24] A.E. Abouelregal, W. Mohammed, WEffects of nonlocal thermoelasticity on nanoscale beams based on couple stress theory, Math. Methods Appl. Sci. (2020), https://doi.org/10.1002/mma.6764.
[25] A.E. Abouelregal, M. Marin, The response of nanobeams with temperature-dependent properties using state-space method via modified couple stress theory, Symmetry 12 (2020) 1276.
[26] A.E. Abouelregal, Size-dependent thermoelastic initially stressed micro-beam due to a varying temperature in the light of the modified couple stress theory, Appl. Math. Mech. -Engl. Ed. 41 (12) (2020) 1805–1820.
[27] A.E. Abouelregal, Response of thermoelastic micro-beams to a periodic external transverse excitation based on MCS theory, Microsyst. Technol. 24 (2018) 1925–1933.
[28] M.M. Benhamed, A.E. Abouelregal, Influence of temperature pulse on a Nickel microbeams under couple stress theory, J. Appl. Comput. Mech. 6 (4) (2020) 777–787.
[29] N. Shafiei, A. Mousavi, M. Ghadiri, Vibration behavior of a rotating non-uniform FG microbeam based on the modified couple stress theory and GDQEM, Compos. Struct. 149 (2016) 157–169.
[30] A.M. Dehrouyeh-Semnani, The influence of size effect on flapwise vibration of rotating microbeams, Int. J. Eng. Sci. 94 (2015) 150–163.
[31] M. Ghadiri, N. Shafiei, Vibration analysis of rotating functionally graded Timoshenko microbeam based on modified couple stress theory under different temperature distributions, Acta Astronaut. 121 (2016) 221–240.
[32] S. Narendar, Mathematical modelling of rotating single-walled carbon nanotubes used in nanoscale rotational actuators, Defence Sci. J. 61 (2011) 317–324.
[33] M. Ghadiri, N. Shafiei, S. Alireza Mousavi, Vibration analysis of a rotating functionally graded tapered microbeam based on the modified couple stress theory by DQEM, Appl. Phys. A 122 (2016) 837.
[34] M. Ghafarian, A. Ariaei, Free vibration analysis of a system of elastically interconnected rotating tapered Timoshenko beams using differential transform method, Int. J. Mech. Sci. 107 (2016) 93–109.
[35] S. Bhattacharya, D. Das, Modified couple stress-based free vibration behavior of pre-twisted tapered BFGM rotating micro beam considering spin-softening and Coriolis effects, Proc. IMechE Part L: J. Mater.: Design Appl. 234 (1) (2020) 21–47.
[36] J. Fang, J. Gu, H. Wang, Size-dependent three-dimensional free vibration of rotating functionally graded microbeams based on a modified couple stress theory, Int. J. Mech. Sci. 136 (2018) 188–199.
[37] M. Malik, D. Das, Free vibration analysis of rotating nano-beams for flap-wise, chord-wise and axial modes based on Eringen's nonlocal theory, Int. J. Mech. Sci. 179 (2020) 105655.
[38] A.E. Abouelregal, H.M. Sedighi, S.A. Faghidian, A.H. Shirazi, Temperature-dependent physical characteristics of the rotating nonlocal nanobeams subject to a varying heat source and a dynamic load, Facta Univ. – Ser. Mech. Eng. (2021), https://doi.org/10.22190/FUME201222024A.
[39] A. Rahmani, B. Safaei, Z. Qin, On wave propagation of rotating viscoelastic nanobeams with temperature effects by using modified couple stress-based nonlocal Eringen's theory, Eng. Comput. (2021), https://doi.org/10.1007/s00366-021-01429-0.
[40] A.E. Abouelregal, H. Ahmad, T.A. Nofal, H. Abu-Zinadah, Thermo-viscoelastic fractional model of rotating nanobeams with variable thermal conductivity due to mechanical and thermal loads, Mod. Phys. Lett. B (2021), https://doi.org/10.1142/S0217984921502973.
[41] A.E. Abouelregal, H. Ahmad, K.A. Gepreeld, P. Thounthong, Modelling of vibrations of rotating nanoscale beams surrounded by a magnetic field and subjected to a harmonic thermal field using a state-space approach, Eur. Phys. J. Plus 136 (2021) 268.
[42] A.E. Abouelregal, H. Ahmad, Thermodynamic modeling of viscoelastic thin rotating microbeam based on non-Fourier heat conduction, Appl. Math. Model. 91 (2021) 973–988.
[43] A.E. Aboueregal, H.M. Sedighi, The effect of variable properties and rotation in a visco-thermoelastic orthotropic annular cylinder under the Moore–Gibson–Thompson heat conduction model, Proc. IMechE Part L: J. Mater.: Design Appl. 235 (5) (2021) 1004–1020.
[44] M. Biot, Thermoelasticity and irreversible thermo-dynamics, J. Appl. Phys. 27 (1956) 240–253.
[45] H. Lord, Y. Shulman, A generalized dynamical theory of thermoelasticity, J. Mech. Phys. Solid. 15 (1967) 299–309.
[46] A.E. Green, K.A. Lindsay, Thermoelasticity. J. Elast. 2 (1972) 1–7.
[47] D.Y. Tzou, Thermal shock phenomena under high rate response in solids, Annu. Rev. Heat Transf. 4 (4) (1992) 111–185.
[48] D.Y. Tzou, The generalized lagging response in small-scale and high-rate heating, Int. J. Heat Mass Tran. 38 (17) (1995) 3231–3240.
[49] D.Y. Tzou, A unified field approach for heat conduction from macro-to micro-scales, J. Heat Tran. 117 (1) (1995) 8–16.
[50] I. Kaur, P. Lata, K. Singh, Reflection and refraction of plane wave in piezo-thermoelastic diffusive half spaces with three phase lag memory dependent derivative and two-temperature, Wav. Rand. Compl. Media (2020), https://doi.org/10.1080/17455030.2020.1856451.
[51] P. Lata, H. Kaur, Time harmonic interactions in the axisymmetric behaviour of transversely isotropic thermoelastic solid using new M-CST, Coupl. Syst. Mech. 9 (6) (2020) 521–538.
[52] P. Lata, I. Kaur, K. Singh, Thermomechanical interactions due to time harmonic sources in a transversely isotropic magneto thermoelastic rotating solids in Lord-Shulman model, Mater. Phys. Mech. 46 (2020) 7–26.
[53] I. Kaur, P. Lata, K. Singh, Study of frequency shift and thermoelastic damping in transversely isotropic nano-beam with GN III theory and two temperature, Arch. Appl. Mech. 91 (2021) 1697–1711.
[54] L.Y. Bahar, R.B. Hetnarski, State space approach to thermoelasticity, J. Therm. Stresses 1 (1978) 135–145.
[55] H. Sherief, State space formulation for generalized thermoelasticity with one relaxation time including heat sources, J. Therm. Stresses 16 (1993) 163–180.
[56] M. Bachher, N. Sarkar, Nonlocal theory of thermoelastic materials with voids and fractional derivative heat transfer, Wav. Rand. Compl. Media 29 (4) (2019) 595–613.
[57] D. Singh, G. Kaur, S.-K. Tomar, Waves in nonlocal elastic solid with voids, J. Elasticity 128 (1) (2017) 85–114.
[58] S. Biswas, Surface waves in porous nonlocal thermoelastic orthotropic medium, Acta Mech. 231 (2020) 2741–2760.
[59] A.R. Hadjesfandiari, G.F. Dargush, Couple stress theory for solids, Int. J. Solid Struct. 48 (18) (2011) 2496–2510.
[60] R. Kumar, Response of thermoelastic beam due to thermal source in modified couple stress theory, CMST 22 (2) (2016) 95–101.
[61] Z.M. Zhang, Nano/Microscale Heat Transfer, McGraw-Hill, USA, 2007.

[62] K.M. Hangos, R. Lakner, M. Gerzson, Intelligent Control Systems: an Introduction with Examples, Springer Science & Business Media, 2006.
[63] A.S. Vasilyev, A.V. Ushakov, Modeling of dynamic systems with modulation by means of Kronecker vector-matrix representation, Sci. Tech. J. Inf. Technol. Mech. Optics 15 (5) (2015) 839–848.
[64] G. Honig, U. Hirdes, A method for the numerical inversion of Laplace Transform, J. Comput. Appl. Math. 10 (1984) 113–132.
[65] A. Cheng, P. Sidauruk, Approximate inversion of the Laplace transform, Math. J. 4 (1994) 76–82.
[66] H. Hassanzadeh, M. Poolad-Darvish, Comparison of different numerical Laplace inversion methods for engineering application, Appl. Math. Comput. 189 (2007) 1966–1981.
[67] H. Sadeghian, H. Goosen, A. Bossche, B. Thijsse, F. van Keulen, On the size-dependent elasticity of silicon nano-cantilevers: impact of defects, J. Phys. D Appl. Phys. 44 (2011), 072001.
[68] Y. Cao, D.D. Nankivil, S. Allameh, W.O. Soboyejo, Mechanical properties of Au films on silicon substrates, Mater. Manuf. Process. 22 (2007) 187–194.
[69] G.Z. Voyiadjis, R.K. Abu Al-Rub, Gradient plasticity theory with a variable length scale parameter, Int. J. Solid Struct. 42 (2005) 3998–4029.
[70] S.K. Jena, S. Chakraverty, M. Malikan, H. Mohammad-Sedighi, Hygro-magnetic vibration of the single-walled carbon nanotube with nonlinear temperature distribution based on a modified beam theory and nonlocal strain gradient model, Int. J. Appl. Mech. 12 (5) (2020) 2050054.
[71] Y. Wang, D. Liu, Q. Wang, J. Zhou, Asymptotic solutions for generalized thermoelasticity with variable thermal material properties, Arch. Mech. 68 (3) (2016) 181–202.
[72] A.E. Aboueregal, H.M. Sedighi, The effect of variable properties and rotation in a visco-thermoelastic orthotropic annular cylinder under the Moore–Gibson–Thompson heat conduction model, Proc. IMechE Part L: J. Mater.: Design Appl. 235 (5) (2021) 1004–1020.
[73] F. Ebrahimi, P. Haghi, Elastic wave dispersion modelling within rotating functionally graded nanobeams in thermal environment, Adv. Nano Res. 6 (3) (2018) 201–217.